THE JOURNAL OF BIOLOGICAL CHEMISTRY VOL. 285, NO. 32, pp. 24740–24750, August 6, 2010

The Interaction with HMG20a/b Proteins Suggests a Potential Role for β-Dystrobrevin in Neuronal Differentiation*[S]

Received for publication, December 1, 2009, and in revised form, May 10, 2010 Published, JBC Papers in Press, June 8, 2010, DOI 10.1074/jbc.M109.090654

Benedetta Artegiani[‡1], Catherine Labbaye[§], Antonella Sferra[‡], Maria Teresa Quaranta[§], Paola Torreri[¶], Gianfranco Macchia[‡], Marina Ceccarini[¶], Tamara C. Petrucci[‡], and Pompeo Macioce[‡2]

From the Departments of [‡]Cell Biology and Neuroscience and [§]Haematology, Oncology, and Molecular Medicine and [¶]National Center for Rare Diseases, Istituto Superiore di Sanità, Rome 00161, Italy

α and β dystrobrevins are cytoplasmic components of the dystrophin-associated protein complex that are thought to play a role as scaffold proteins in signal transduction and intracellular transport. In the search of new insights into the functions of β-dystrobrevin, the isoform restricted to non-muscle tissues, we performed a two-hybrid screen of a mouse cDNA library to look for interacting proteins. Among the positive clones, one encodes iBRAF/HMG20a, a high mobility group (HMG)-domain protein that activates REST (RE-1 silencing transcription factor)-responsive genes, playing a key role in the initiation of neuronal differentiation. We characterized the β-dystrobrevin-iBRAF interaction by *in vitro* and *in vivo* association assays, localized the binding region of one protein to the other, and assessed the kinetics of the interaction as one of high affinity. We also found that β-dystrobrevin directly binds to BRAF35/HMG20b, a close homologue of iBRAF and a member of a co-repressor complex required for the repression of neural specific genes in neuronal progenitors. *In vitro* assays indicated that β-dystrobrevin binds to RE-1 and represses the promoter activity of synapsin I, a REST-responsive gene that is a marker for neuronal differentiation. Altogether, our data demonstrate a direct interaction of β-dystrobrevin with the HMG20 proteins iBRAF and BRAF35 and suggest that β-dystrobrevin may be involved in regulating chromatin dynamics, possibly playing a role in neuronal differentiation.

Dystrobrevin is a cytoplasmic component of the dystrophin-associated protein complex (DPC),[3] a membrane complex that links the cortical actin cytoskeleton to the extracellular matrix (1) and serves as a scaffold for signaling proteins (2). Defects in DPC function and assembly cause several forms of muscular dystrophy (3), a group of genetic diseases affecting skeletal, smooth, and cardiac muscles, and in some cases involving the central nervous system. Indeed, many patients with muscular dystrophy suffer from cognitive impairment, learning disability, and neuropsychiatric disorders (4); the brain dysfunction is thought to be a non-progressive disorder that occurs early, probably during embryogenesis, whereas the muscle disease arises later and is progressive (5, 6).

Dystrobrevins are the product of two different genes coding for two highly homologous proteins, α- and β-dystrobrevin (7, 8). Several distinct transcripts are derived from each gene by alternative promoter usage and alternative splicing, generating a large family of dystrobrevin isoforms (9–11). α-Dystrobrevin is expressed predominantly in skeletal muscle, heart, lung, and brain (9, 12), whereas β-dystrobrevin is restricted to non-muscle tissues and is abundantly expressed in brain, lung, kidney, and liver (10, 11). Mice lacking α-dystrobrevin have a mild form of muscular dystrophy, which does not impair the DPC assembly (13), whereas mice lacking β-dystrobrevin appear to be phenotypically normal, although alterations of dystrophin Dp71 and syntrophin isoforms at the basal membranes of kidney and liver can be observed (14). However, double knock-out mice lacking both α- and β-dystrobrevin reveal a decrease in the size and number of γ-aminobutyric acid receptor clusters at cerebellar inhibitory synapses, loss of dystrophin from these sites, and sensorimotor behaviors that reflect perturbations in cerebellar function (15). Dystrobrevin double knock-out mice, therefore, provided evidence that DPC components other than dystrophin affect synaptic structure in the brain, suggesting that motor deficits in dystrophic patients may reflect not only peripheral derangements but also central nervous system defects (15). The role of dystrobrevins remains elusive, although their cellular functions are beginning to be elucidated through the study of their associated proteins. Several dystrobrevin-associated proteins have recently been described, including dysbindin (16), kinesin (17, 18), DAMAGE (19), protein kinase A (20), and pancortin (21). Among these, pancortin has been proposed to support neuronal differentiation and survival (22), and dysbindin has been indicated as a schizophrenia susceptibility gene (23), suggesting that dystrobrevin might be involved in cognitive defects and neuropsychiatric disorders.

Here we characterized the association of β-dystrobrevin with a novel binding partner, the high mobility group (HMG) protein iBRAF/HMG20a, and found that β-dystrobrevin also interacts with the close homologue of iBRAF, BRAF35/HMG20b. HMG proteins are ubiquitous non-histone proteins that bind to DNA and chromatin, acting as architectural ele-

* This work was supported in part by the Italy-USA Collaborative Programme (Grant Rare Diseases, 7DR1).

[S] The on-line version of this article (available at http://www.jbc.org) contains supplemental Fig. S1.

[1] Present address: Center for Regenerative Therapies, Dresden 01307, Germany.

[2] To whom correspondence should be addressed: Dept. of Cell Biology and Neuroscience, Istituto Superiore di Sanità, Viale Regina Elena 299, 00161 Rome, Italy. Tel.: 390649902075; Fax: 390649387143; E-mail: pompeo.macioce@iss.it.

[3] The abbreviations used are: DPC, dystrophin-associated protein complex; HMG, high mobility group; RE-1, repressor element-1; REST, RE-1 silencing transcription factor; GST, glutathione *S*-transferase; Ni-NTA, nickel-nitrilotriacetic acid; SPR, surface plasmon resonance; β-DB, β-dystrobrevin; RU, response units; HA, hemagglutinin.

ments that modulate chromatin structure, and control the expression of a number of genes (24). We also report that β-dystrobrevin binds to and represses the promoter of synapsin I, a neuronal differentiation gene. Our results corroborate the role of dystrobrevin as a multifunctional scaffold protein and suggest that in neurons it might be involved in differentiation processes as a component of co-activator/co-repressor complexes required for the regulation of neural-specific genes.

EXPERIMENTAL PROCEDURES

Antibodies—A goat HMG20a polyclonal antibody (Everest Biotech) was used to detect iBRAF/HMG20a. A dystrobrevin monoclonal antibody (Clone 23, BD Transduction Laboratories) or a polyclonal antibody raised against β-dystrobrevin (17) were used to detect dystrobrevins. Additional antibodies used were GATA-4 (H-112) polyclonal antibody (Santa Cruz Biotechnology), c-Myc tag (Clontech), and BRAF35 (4.21) (Santa Cruz Biotechnology) monoclonal antibodies.

Plasmid Constructs—Construction of pGEX-6P/β-DB, pGBKT7/β-DB, pGADT7/β-DB, and pCMV-HA/β-DB is described in detail elsewhere (17) as is construction of pCRII-TOPO/α-DB1 (18), pCRII-TOPO/β-DB_{1-352}, and pCRII-TOPO/β-$DB_{357-615}$ (21) and of pCMV-Myc/β-DB (20). pEGFP-C2/β-DB, pGEX-6P/β-DB_{1-352}, and pGEX-6P/β-$DB_{357-615}$ were obtained by EcoRI digestion of pGBKT7/β-DB, pCRII-TOPO/β-DB_{1-352}, and pCRII-TOPO/β-$DB_{357-615}$, respectively, and insertion of the corresponding insert into the EcoRI site of pEGFP-C2 (BD Biosciences Clontech) and pGEX-6P-1 (Amersham Biosciences). The DNA insert coding for the iBRAF carboxyl-terminal region (amino acids 233–342) and the upstream hemagglutinin (HA) epitope tag was amplified by PCR from the pACT2-iBRAF template and subcloned into pCRII-TOPO and into pEXP5-NT-TOPO (Invitrogen) to create pCRII-TOPO/$iBRAF_{233-342}$ and pEXP5-NT-TOPO/$iBRAF_{233-342}$, respectively. The whole coding region of iBRAF was obtained by PCR amplification of reverse-transcribed RNA isolated from mouse brain using specific primers that annealed at the 5′ and 3′ regions overlapping the start and stop codon, respectively. The 1.0-kb full-length iBRAF sequence was then cloned into pCRII-TOPO and pEXP5-NT-TOPO vectors to obtain pCRII-TOPO/iBRAF and pEXP5-NT-TOPO/iBRAF, respectively. Full-length iBRAF was then amplified by PCR from pCRIITOPO/iBRAF with a 5′ artificial XhoI site and a 3′ artificial HindIII site and subcloned into the XhoI-HindIII sites of pDsRed-Monomer-C1 (BD Biosciences Clontech) to produce pDsRed-C1/iBRAF. pCMV-HA/iBRAF and pCMV-Myc/iBRAF were obtained by XhoI-KpnI digestion of pDsRed-C1/iBRAF and insertion of the iBRAF fragment into the XhoI-KpnI of pCMV-HA and pCMV-Myc vectors (BD Biosciences Clontech). The full-length coding region of BRAF35 was cloned by reverse transcription-PCR from mouse brain into pCRII-TOPO vector to obtain pCRII-TOPO/BRAF35. After EcoRI digestion, the BRAF35 fragment was inserted into the EcoRI site of pGEX-6P-1 (Amersham Biosciences) to create pGEX-6P/BRAF35. Full-length human Dp71 cDNA, obtained as reported previously (25), was subcloned into pCRII-TOPO to produce pCRII-TOPO/Dp71. A 466-bp DNA fragment of the human synapsin I promoter (from −422 to + 44) containing the RE-1 sequence was amplified by PCR from pSyCAT-10 (26), with a 5′ artificial XhoI site and a 3′ artificial NotI site, and subcloned into pCRII-TOPO to create pCRII-TOPO/SYN. A 520-bp fragment obtained after XhoI digestion of pCRII-TOPO/SYN was then inserted into the XhoI site upstream of the luciferase gene of the pGL3-Promoter vector (pGL3-Prom; Promega) to obtain pGL3-Prom/SYN. All constructs were checked by sequence analysis.

In Vitro Transcription and Translation—TNT SP6 or T7 Quick Coupled Transcription/Translation System (Promega) in the presence of PRO-MIX (70% L-[^{35}S]methionine; 30% L-[^{35}S]cysteine; Amersham Biosciences) was used to transcribe and translate *in vitro* pCRII-TOPO/iBRAF and pCRII-TOPO/$iBRAF_{233-342}$ to obtain ^{35}S-labeled full-length iBRAF and the amino-terminal truncated mutant $iBRAF_{233-342}$, respectively. The same procedure was followed for pCRII-TOPO/β-DB and deletion mutants pCRII-TOPO/α-DB1 and pCRII-TOPO/Dp71 to obtain the corresponding polypeptides. Newly synthesized proteins were separated by SDS-PAGE and analyzed with an Instant-Imager (Packard Instrument Co.).

Protein Pulldown Assays—β-Dystrobrevin full-length and deletion mutants as well as BRAF35 were obtained as recombinant GST-fused proteins from the corresponding constructs in pGEX-6P and used to perform GST pulldown as previously described using 150 mM NaCl, 5 mM $MgSO_4$, 1 mM dithiothreitol, 0.2% Triton X-100, 20 mM Hepes, pH 7.4, and protease inhibitors as binding buffer (20). Recombinant His_6-iBRAF and His_6-$iBRAF_{233-342}$ were obtained from pEXP5-NT-TOPO/iBRAF and pEXP5-NT-TOPO/$iBRAF_{233-342}$, respectively. For His_6 pulldown, amino-terminal polyhistidine (His_6)-fused proteins were expressed in *Escherichia coli* BL21-DE3-pLysS (His_6-iBRAF) and BL21-DE3 (His_6-$iBRAF_{233-342}$) cells, respectively, and purified by affinity chromatography on Ni-NTA-agarose beads (Qiagen) following the manufacturer's instructions. His_6 fusion proteins bound to Ni-NTA-agarose beads were equilibrated in binding buffer (150 mM NaCl, 10 mM imidazole, 2 mM EDTA, 0.05% Triton X-100, 20 mM Tris-HCl, pH 7.5, and protease inhibitors). For binding assays, 5–20 μl of *in vitro* translated reaction products were incubated with 10–20 μl of 50% slurry bead-bound His_6 fusion proteins overnight at 4 °C on a rotator. After extensive washes with binding buffer, bound radioactive proteins were re-suspended in Laemmli loading buffer and separated by SDS-PAGE. Gels were dried, and radiolabeled proteins were detected by autoradiography.

Surface Plasmon Resonance Experiments—Surface plasmon resonance (SPR) analysis was performed using a BIAcoreX instrument (BIAcore Intl. AB) equipped with two flow-cell sensor chips, basically as described previously (20). The interaction of His_6-iBRAF and His_6-BRAF35 with β-dystrobrevin was studied with a dextran matrix CM5 sensor chip at 25 °C. Immobilization of the proteins was achieved by covalently coupling the proteins to CM5 sensor chips after activation of the carboxymethylated dextran surface by a mixture of 0.05 M *N*-hydroxysuccinimide and 0.2 M *N*-ethyl-*N*′-3-(dimethylaminopropyl) carbodiimide hydrochloride. The reaction was performed by injecting His_6-iBRAF or His_6-BRAF35 in 10 mM acetate buffer, pH 4.8 or 5.2, respectively, and then blocking the residual activated groups with 1 M ethanol-

amine-HCl, pH 8.5. The reference cell surface was subjected to the same procedure without the protein. Experiments were performed in HBS-EP (150 mM NaCl, 3 mM EDTA, 10 mM Hepes, pH 7.4, 0.005% (v/v) surfactant P20) with a flow rate of 30 μl/min. Full-length β-dystrobrevin, obtained by digestion with PreScission protease (Amersham Biosciences) (18), was applied in triplicate injections of each concentration. β-Dystrobrevin-truncated mutants, obtained as above, were applied by injections at the concentration of 2 μM, always in triplicate.

The amount of protein bound to the sensor chip was monitored by changes in the refractive index, given in arbitrary response units (RU) as a function of time (sensorgram). At the end of the sample plug, HBS-EP buffer was passed over the sensor surface for 4 min to allow dissociation. The sensor surface was regenerated for the next sample using a 5-μl pulse of 50 mM NaOH at a flow rate of 30 μl/min and running buffer until the initial RU level was regained. Injecting β-dystrobrevin samples at the same concentration at the beginning and at the end of a set of experiments resulted in the same RU value, indicating that the ligand was not altered by the chip regeneration process. SPR data were analyzed using the Langmuir model for 1:1 binding and the BIAevaluation software Version 4.1 as described (18). The dissociation rate constant k_{off} was evaluated from curves obtained at the saturation of β-dystrobrevin and used to calculate the association rate constant k_{on} and the dissociation constant ($K_d = k_{off}/k_{on}$). Alternatively, the K_d was evaluated using BIAevaluation 4.1 software to simultaneously fit sensorgrams.

Cell Culture and Fluorescence Microscopy—Human pluripotent embryonal carcinoma cells NTera-2, clone Dl (NTera-2), were grown at 37 °C in Dulbecco's modified Eagle's medium (high glucose formulation) supplemented with 10% fetal calf serum (Invitrogen) in a 5% CO_2 in air, humidified atmosphere. NTera-2 cells were maintained in their undifferentiated phenotype by continuous growth at high cell density (5–50 × 10^6 cells/175 cm^2 flask), and differentiation was induced by seeding cells at 2 × 10^6 cells per 175-cm^2 flasks in 10^{-6} M retinoic acid (Sigma) as described (28). P19 cells were grown in α-modified minimal essential medium (Invitrogen) containing 7.5% heat-inactivated newborn calf serum (Invitrogen) and 2.5% fetal bovine serum (Invitrogen) and split 20 times every other day using 0.05% trypsin-0.02% EDTA as previously described (29). HeLa and COS-7 cells were grown and maintained (5% CO_2, 37 °C) in Dulbecco's modified Eagle's medium supplemented with 10% fetal bovine serum. COS-7 cells seeded on sterile, untreated glass coverslips were transiently transfected using FuGENE 6 (Roche Applied Science) according to the manufacturer's instructions. At 24 h after transfection, the cells were washed with Tris-buffered saline, fixed with 3.7% formaldehyde in Tris-buffered saline for 15 min at room temperature and incubated for 10 min with 1 μg/ml Hoechst 3342 to stain nuclei. Cells were then mounted with VectaShield (Vector Laboratories), and green (enhanced green fluorescent protein), red (DsRed), and blue (Hoechst) fluorescence signals were examined under a Leica TCS 4D confocal microscope. Image acquisition and processing were performed using the SCANware and Multicolor Analysis (Leica Lasertechnik Gmbh) and Adobe Photoshop (Adobe Systems) software programs.

Pulldown Experiments and Immunoprecipitation from Lysates—Tissue from rat brain was homogenized as described elsewhere (20). For the His_6 pulldown assays, 1 mg of proteins from rat brain lysate in 0.7 ml of binding buffer (150 mM NaCl, 10 mM imidazole, 2 mM EDTA, 0.05% Triton X-100, 20 mM Tris-HCl, pH 7.5, and protease inhibitors) was cleared by centrifugation at 100,000 × *g* for 30 min at 4 °C. The precleared supernatant was then incubated for 2 h with 5 μl of 50% slurry bead-bound His_6-iBRAF, and the beads were washed 6 times with 0.5 ml of binding buffer. Ni-NTA-agarose beads were used as control. After washing, the samples were subjected to SDS-PAGE, transferred to a nitrocellulose membrane, and immunoblotted with the β-dystrobrevin polyclonal antibody. For the co-immunoprecipitation experiments, 3 mg of proteins from rat brain lysate in 0.25 ml of lysis buffer (20 mM NaCl, 5 mM EDTA, 5 mM EGTA, 0.5% Triton X-100, 1 mM dithiothreitol, 20 mM Hepes, pH 7.4, and protease inhibitors) was centrifuged at 100,000 × *g* for 30 min, and the supernatant was preincubated for 2 h at 4 °C with 30 μl of recombinant protein G-agarose (Invitrogen) (50% slurry) to minimize nonspecific binding. After centrifugation, 1.25 μg of dystrobrevin monoclonal antibody was added to the lysate, and the sample was rotated at 4 °C overnight. 30 μl of recombinant protein G-agarose gel were then added, and incubation was continued for 2h at 4 °C. Beads were washed 6 times with ice-cold Tris-buffered saline-Tween (150 mM NaCl, 1 mM dithiothreitol, 20 mM Tris-HCl, pH 7.5, 0.1% Tween 20, and protease inhibitors). After washing, the samples were subjected to SDS-PAGE, transferred to a nitrocellulose membrane, and immunoblotted with the HMG20a polyclonal antibody or with the polyclonal β-dystrobrevin antibody. Co-immunoprecipitation studies on COS-7 cells were performed essentially as follows. Briefly, COS-7 cells were transiently transfected with pCMV-Myc/iBRAF or pCMV-HA/iBRAF and lysed in a buffer containing 150 mM NaCl, 1% Triton X-100, 0.5% sodium deoxycholate, 50 mM Tris-HCl, pH 7.4, and protease inhibitors. 0.4 ml of precleared lysates (1 mg/ml) was then incubated overnight at 4 °C with the c-Myc monoclonal antibody or HA-tag polyclonal antibody (Clontech) and immunoprecipitated using 30 μl of recombinant protein G-agarose. After extensive washing, samples were separated by SDS-PAGE and transferred to nitrocellulose. Blots were then probed with the goat polyclonal HMG20a antibody and the rabbit polyclonal β-dystrobrevin antibody. Bound antibodies were visualized by using the ECL system (Pierce).

Electrophoretic Mobility Shift Assay—Electrophoretic mobility shift assays were performed as previously reported (30). Each binding reaction (20 μl) contained 10 μg of NTera-2 cells nuclear extracts after 4 days of retinoic acid treatment in a buffer, pH 7.5, of 20 mM $ZnCl_2$, 10 mM Tris-HCl, 10 mM $MgCl_2$, 75 mM NaCl, 1 mM dithiothreitol, poly(dI/dC), and bovine serum albumin (500 ng per sample), 10% glycerol, and a 30,000 cpm/sample ^{32}P-labeled double-strand oligonucleotide probe encompassing the 21-bp synapsin RE-1 element (RE-1^*_{syn}) 5′-CAGCTTCAGCACCGCGGACAGTGCCTTC-3′ (from −237 to −210 bp from the first nucleotide in the proximal synapsin I promoter sequence) (31). After 45 min on ice, the protein-DNA

complexes were resolved in a 5% polyacrylamide gel and visualized by autoradiography. A 50-, 100-, 300-, 600-fold molar excess of unlabeled oligonucleotide probe (RE-1_{SYN}) or unlabeled mutated oligonucleotide probe (RE-1_{Mut}) 5′-CAGCGTCGGTAGCCCTGGCTGAGCGTTC-3′ was used for competition experiments. 3 μg of the β-dystrobrevin polyclonal antibody or the GATA-4 polyclonal antibody as a negative control were used for supershift assay.

Luciferase Assay—In luciferase assays COS-7 cells were cotransfected with pGL3-Prom/SYN and pRL-TK control plasmid (Promega) containing the herpesvirus thymidine kinase promoter linked to the *Renilla* luciferase gene in a ratio of 10:1 using Lipofectamine 2000 (Invitrogen). Where indicated, pCMV-myc/Empty, pCMV-myc/iBRAF, or pCMV-myc/β-DB were also transfected. The empty pGL3-Promoter vector (pGL3-Prom; Promega), which contains the SV40 promoter upstream of firefly luciferase gene but lacks enhancer elements, was used as an internal standard for promoter activity. Luciferase activity was measured 48 h post-transfection using the Dual Luciferase Reporter System (Promega) and the Microlite TLX1 luminometer (Dynatech Laboratories) and normalized for *Renilla* luciferase activity. Data are presented as the mean values ± S.E. obtained from at least three independents experiments.

RESULTS

Identification of iBRAF as a Binding Partner of β-Dystrobrevin—We previously described a two-hybrid mating screen performed to identify proteins that interact with β-dystrobrevin (β-DB) in the brain (17). End sequencing and BLAST searching of positive clones revealed that one of them contained the coding sequence of the carboxyl-terminal region (amino acids 233–342) of iBRAF/HMG20a (GenBank™ accession no. ABA26278), an HMG protein with close sequence and structural homology to BRAF35/HMG20b, a member of the BRAF35-HDAC complex that has a key role in the repression of neural specific genes in neuronal progenitors (32). In contrast to BRAF35, iBRAF expression leads to the initiation of neuronal differentiation (33).

We have confirmed the $iBRAF_{233–342}$/β-dystrobrevin interaction in the yeast system by mating MATa strain AH109 transformed with pACT2/$iBRAF_{233–342}$ with MATα strain Y187 transformed with pGBKT7/β-DB. $iBRAF_{233–342}$ interacts with β-dystrobrevin but not with the unrelated protein lamin C, nor does it transactivate reporter gene expression (data not shown).

We tested recombinant GST-β-dystrobrevin for interaction with ^{35}S-labeled carboxyl-terminal $iBRAF_{233–342}$ (Fig. 1*A*). Pulldown experiments confirmed that a binding site for β-dystrobrevin lies on the iBRAF carboxyl-terminal region (Fig. 1*B*), as indicated by the two-hybrid system results.

In Vitro Association of β-Dystrobrevin and iBRAF—iBRAF full-length recombinant protein was obtained by reverse transcription-PCR and subsequent subcloning into the appropriate vector. The direct interaction between iBRAF and β-dystrobrevin was confirmed by pulldown experiments performed with either full-length His_6-iBRAF and *in vitro* transcribed/translated β-dystrobrevin (Fig. 2*A*, *left*) or GST-β-dystrobrevin and *in vitro*-transcribed/translated iBRAF (Fig. 2*A*, *right*). No interaction with dysbindin (*Dysb*) or GST protein, respectively, used as negative controls, was detected (Fig. 2*A*). Considering the high level of sequence homology between β- and α-DB, we wondered whether iBRAF could interact with α-dystrobrevin as well. Interestingly, we found that His_6-iBRAF failed to interact with *in vitro* transcribed/translated α-dystrobrevin (Fig. 2*B*), suggesting that the association with iBRAF is specific for the β isoform of dystrobrevin.

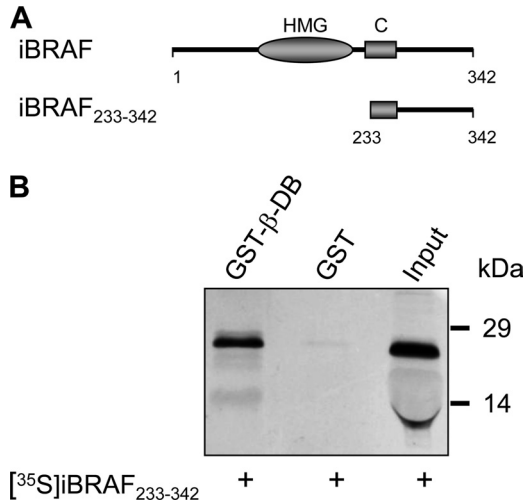

FIGURE 1. **Direct interaction of β-dystrobrevin with the carboxyl-terminal region of iBRAF *in vitro*.** *A*, shown is a schematic representation of full-length iBRAF and the iBRAF-carboxyl terminus used in the pulldown assay. The positions of the HMG-box (*HMG*) and the coiled-coil region (*C*) are shown. *B*, binding of ^{35}S-labeled carboxyl-terminal iBRAF to immobilized GST-β-dystrobrevin (*GST-β-DB*) is shown. Aliquots of *in vitro* transcribed and translated proteins (*input*) and the proteins pulled down by GST-β-DB or GST immobilized on glutathione-Sepharose beads were analyzed by SDS-PAGE and detected by autoradiography. Molecular mass markers are indicated at the *right* (kDa).

To further characterize this association, we determined the kinetic parameters governing the interaction of β-dystrobrevin with iBRAF by SPR analysis using His_6-iBRAF as ligand and β-dystrobrevin as analyte. Preliminary experiments showing a high nonspecific binding of β-dystrobrevin on NTA surface brought us to choose a CM5 sensor chip. Typical sensorgrams for the binding are shown in Fig. 3. The dissociation rate constant k_{off} (1.08 (±0.1) × 10^{-3} s^{-1}) and the association rate constant k_{on} (3.41 (±0.06) × 10^4 $M^{-1}s^{-1}$) were evaluated from the differential binding curves, assuming an A + B = AB association type. The value of K_d (k_{off}/k_{on}) calculated from different experiments was in the range of 20–40 nM, which indicates an interaction of high affinity.

To identify the region of interaction of iBRAF on β-dystrobrevin, we used ^{35}S-labeled amino-terminal (β-$DB_{1–352}$) and carboxyl-terminal (β-$DB_{357–615}$) β-dystrobrevin mutants (Fig. 4*A*) and tested them for interaction with recombinant His_6-iBRAF. The β-dystrobrevin amino-terminal mutant was pulled down by His_6-iBRAF, whereas the carboxyl-terminal mutant was not (Fig. 4*B*, *left panel*). These data matched the results of an analogous experiment where ^{35}S-labeled iBRAF was pulled down by the GST amino-terminal β-dystrobrevin mutant (Fig. 4*B*, *right panel*). SPR measurements (Fig. 4*C*) and far Western blotting (supplemental Fig. S1) added further evidence that the β-dystrobrevin amino-terminal region is involved in the interaction with iBRAF.

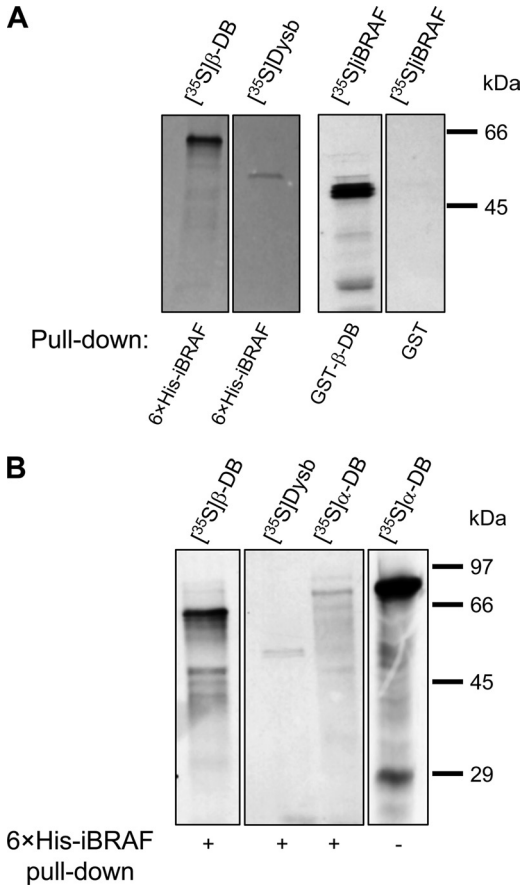

FIGURE 2. **Specific interaction of β-dystrobrevin and full-length iBRAF *in vitro*.** *A*, *left*, binding of ^{35}S-labeled β-DB to histidine-tagged full-length iBRAF (*6×His-iBRAF*) immobilized on Ni-NTA beads is shown; ^{35}S-labeled dysbindin (*Dysb*), a protein unrelated to iBRAF, was used as the negative control. *Right*, binding of ^{35}S-labeled full-length iBRAF to immobilized GST-β-DB; GST protein was used as the negative control. *B*, ^{35}S-labeled α-dystrobrevin 1 did not bind to His_6-iBRAF, indicating that iBRAF interacts specifically with the β-dystrobrevin isoform. β-DB and Dysb were used as positive and negative controls, respectively. Samples were pulled down by the appropriate tagged proteins, analyzed by SDS-PAGE, and detected by autoradiography. Molecular mass markers are indicated at the *right* (kDa).

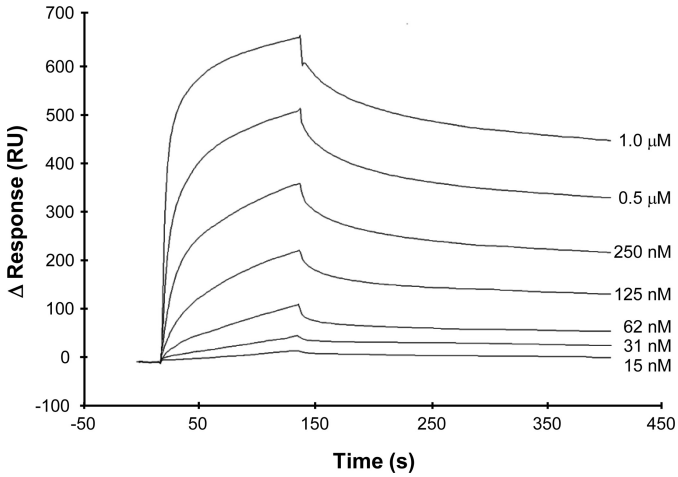

FIGURE 3. **Surface plasmon resonance analysis of β-dystrobrevin interaction with iBRAF.** Increasing concentrations of β-dystrobrevin ranging between 15 nM and 1 μM were allowed to flow over a sensor chip on which His_6-iBRAF had been immobilized. Typical sensorgrams for the binding are shown. The upward slope of each curve corresponds to the signals (RU) observed when the sensor chip was injected with β-dystrobrevin; the downward slope of each curve corresponds to the dissociation of bound β-dystrobrevin after the sample volume has finished flowing and the buffer resumes flowing on the sensor surface. The response (*RU, y axis*) was monitored as a function of time (*s, x axis*) at 25 °C as the difference (Δ) of signals arising from the cell with immobilized His_6-iBRAF and the reference cell. The sensorgrams are representative of triplicate injections.

Immunolocalization of β-Dystrobrevin and iBRAF in Transfected COS-7 Cells—The *in vivo* association of β-dystrobrevin with iBRAF was studied by overexpressing both proteins in COS-7 cells. We first determined the distributions of β-dystrobrevin and iBRAF by single transfection of pEGFP/β-DB or pDsRed-C1/iBRAF. Under confocal microscopy, the transfected β-dystrobrevin displayed an intense punctate staining pattern distributed throughout the cytoplasm (Fig. 5*A*, *a* and *b*), as previously reported (17). In addition, we observed green fluorescence in the nucleus of many transfected cells (Fig. 5*Aa*), indicating that some β-dystrobrevin is also present in the nuclear compartment. Interestingly, red fluorescence of cells transiently transfected with pDsRed-C1/iBRAF showed that iBRAF, which has been described as a nuclear protein (34), can also be expressed in the cytoplasm (Fig. 5*Ad*).

When the constructs encoding iBRAF and β-dystrobrevin were co-transfected, confocal microscopy of the coexpressed proteins indicated that the fluorescence pattern of each protein was changed by the partner protein coexpression (Fig. 5*B*) into structures that can be localized in the nucleus (Fig. 5*B*, *e* and *f*) as well as in the cytoplasm (Fig. 5*B*, *g* and *h*). In these structures, whether β-dystrobrevin and iBRAF showed a different (Fig. 5*B*, *e* and *f*) or a similar amount of expression (Fig. 5*B*, *g* and *h*), they exhibited a significant colocalization, strengthening the hypothesis of their association in a living system. The same results were obtained by immunofluorescence labeling of pCMV-HA/β-DB and pCMV-Myc/iBRAF co-transfected cells, visualized by the suitable anti-tag antibody followed by Alexafluor secondary antibody (not shown).

In Vivo Association of β-Dystrobrevin and iBRAF—We investigated the interaction of β-dystrobrevin and iBRAF *in vivo* also by performing co-precipitation experiments on lysates from COS-7 cells transfected with either pCMV-Myc- or -HA-tagged iBRAF. We used a monoclonal cMyc antibody to co-precipitate Myc-iBRAF and their associated proteins from COS-7-transfected cells and found that β-dystrobrevin co-precipitated with Myc-iBRAF. The polyclonal dystrobrevin antibody used for Western blot is reactive to all dystrobrevin isoforms (α-dystrobrevin 1, 78 kDa; α-dystrobrevin 2, 55 kDa; β-dystrobrevin, 59 kDa; Fig. 6, *COS-7*), but α-dystrobrevin was not detected in the complex co-immunoprecipitated with Myc-iBRAF (Fig. 6). By using a monoclonal dystrobrevin antibody, we found that HA-iBRAF co-precipitated with dystrobrevin in HA-iBRAF-transfected cells (not shown).

We next performed immunoprecipitation and pulldown experiments to ascertain whether the interaction between β-dystrobrevin and iBRAF takes place also in brain. Our results showed that the monoclonal anti-dystrobrevin antibody co-immunoprecipitates iBRAF with the dystrobrevin isoforms from rat brain lysates (Fig. 7*A*). Furthermore, His_6-iBRAF specifically co-precipitated β-dystrobrevin in pulldown experiments on rat brain lysates (Fig. 7*B*). Our polyclonal β-dystrobrevin antibody, which recognizes also the α-dystrobrevin isoforms (17), failed to detect the presence

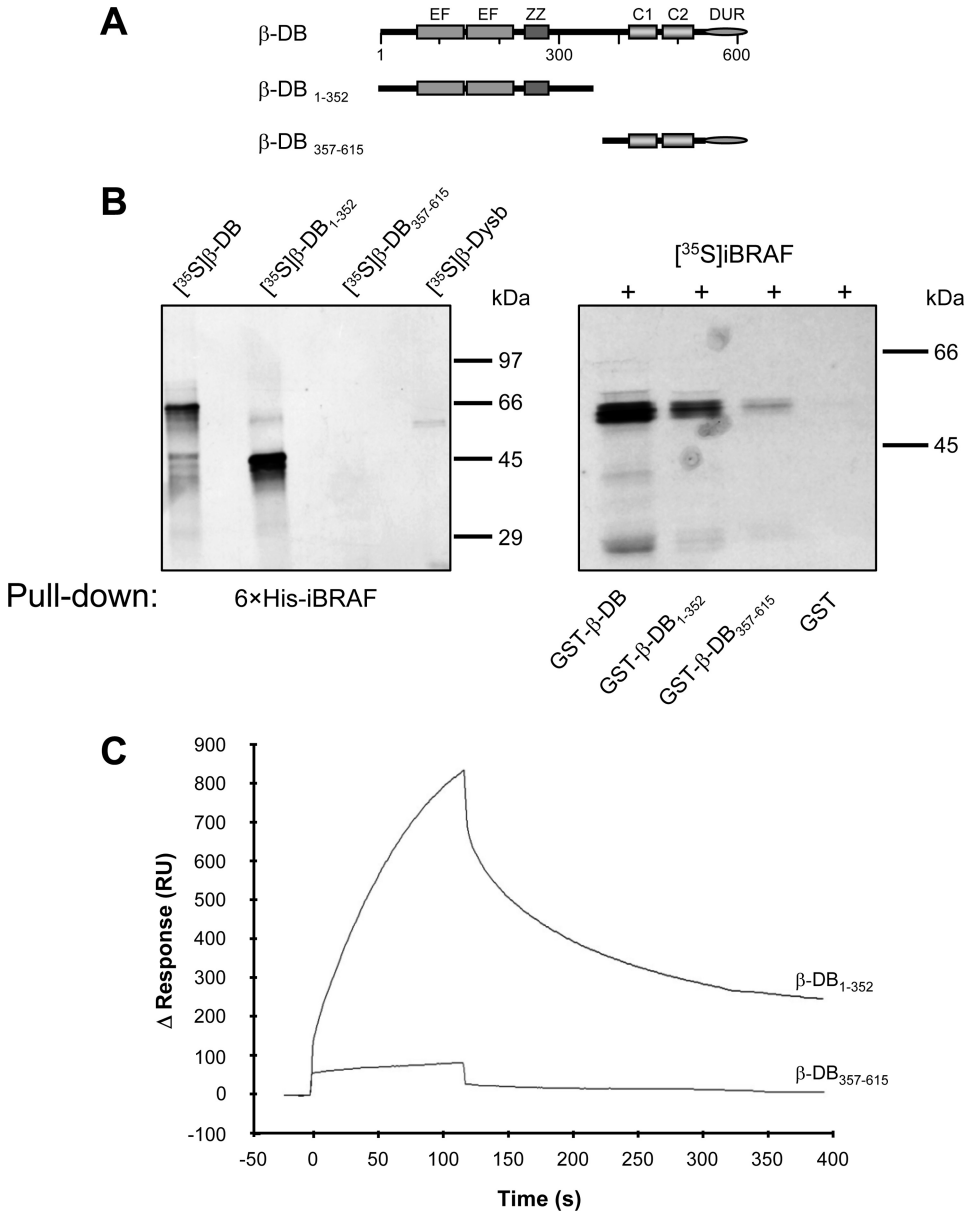

FIGURE 4. **Analysis of β-dystrobrevin regions involved in the interaction with iBRAF.** *A*, shown is s schematic representation of full-length β-dystrobrevin and β-dystrobrevin truncated proteins used in the pull-down assay. The positions of EF-hand (*EF*) motifs, the ZZ domain (*ZZ*), and the two coiled-coil regions (*C1*, *C2*) are shown. *B*, *left*, binding of ^{35}S-labeled β-dystrobrevin and its truncated proteins to immobilized His_6-iBRAF is shown; *Dysb*, negative control. *Right*, binding of ^{35}S-labeled iBRAF to immobilized GST-β-dystrobrevin full-length and truncated proteins is shown; *GST* protein, negative control. Pulled-down proteins were analyzed by SDS-PAGE and detected by autoradiography. Molecular mass markers are indicated at the *right* (*kDa*). *C*, sensorgrams of β-dystrobrevin-truncated proteins (2 μM) on immobilized iBRAF are shown. The response (*RU*, *y axis*) was monitored as a function of time (*s*, *x axis*) at 25 °C as the difference (Δ) of signals arising from the cell with immobilized His_6-iBRAF and the reference cell. The sensorgrams are representative of triplicate injections.

of α-dystrobrevin among the proteins pulled down by His_6-iBRAF (Fig. 7*B*), confirming the data we obtained *in vitro* and from immunoprecipitation experiments on COS-7-transfected cells.

β-Dystrobrevin Is Recruited to RE-1 and Represses the Synapsin I Promoter—Because iBRAF has recently been described as a transcriptional activator of neuronal genes (33), we investigated whether the interaction with β-dystrobrevin may have a role in the regulation of neuronal gene expression. To this aim, we performed electrophoretic mobility shift assays using an oligonucleotide (RE-1_{SYN}) corresponding to the synapsin neuron restrictive silencer element/repressor element-1 (RE-1), a functional binding site for RE-1 silencing transcription factor (REST) (31), BRAF35, and iBRAF (33).

Incubation of labeled synapsin RE-1 probe (RE-1^{*}_{syn}) with nuclear extract from NTera-2 cells after 4 days of retinoic acid treatment led to the formation of a major protein-DNA complex (Fig. 8*A*, *lane 2*). Using the β-dystrobrevin polyclonal antibody, we could not detect a supershift of the complex but did detect a marked decrease of the protein-DNA complex (Fig. 8*A*, *lane 3*), as compared with the complex formation without antibody (Fig. 8*A*, *lane 2*) or with an unrelated monoclonal GATA-4 (G-4) antibody (Fig. 8*A*, *lane 4*), suggesting the presence of the β-dystrobrevin protein in the DNA binding complex. Using competition electrophoretic mobility shift assay analysis, the protein-DNA complex (Fig. 8*A*, *lane 2*) was competed by increasing amounts (50×, 100×, 300×, 600× molar excess) of wild-type unlabeled oligonucleotide (RE-1_{SYN}; Fig. 8*A*, *lanes 5–8*) but not by increasing molar amounts of unlabeled oligonucleotide in which the RE-1 site was mutated (RE-1_{Mut}; Fig. 8*A*, *lanes 9–12*). Altogether our data indicate that β-dystrobrevin participates to a protein complex that binds to synapsin RE-1.

To examine the nature of the interaction between β-dystrobrevin and the promoter of the synapsin I gene, we subcloned a 466-bp fragment of the synapsin I promoter containing the RE-1 sequence (SYN) into the reporter vector pGL3-Promoter (pGL3-Prom) and performed luciferase assays. As expected (31), we observed a 2-fold increase in the pGL3-Prom/SYN luciferase activity compared with the pGL3-Prom basal level, indicating that SYN enhances the activity of the promoter of pGL3-Prom vector (data not shown). In line with previous reports (33), we observed a further increase in pGL3-Prom/SYN luciferase activity when pCMV-iBRAF was co-transfected (Fig. 8*B*). In the presence of β-dystrobrevin, we found a 30% repression of the pGL3-Prom/SYN luciferase activity (Fig. 8*B*), indicating that RE-1 is a β-dystrobrevin DNA binding site and that β-dystrobrevin functions as a repressor of the synapsin I promoter in the pGL3-Prom/SYN reporter system.

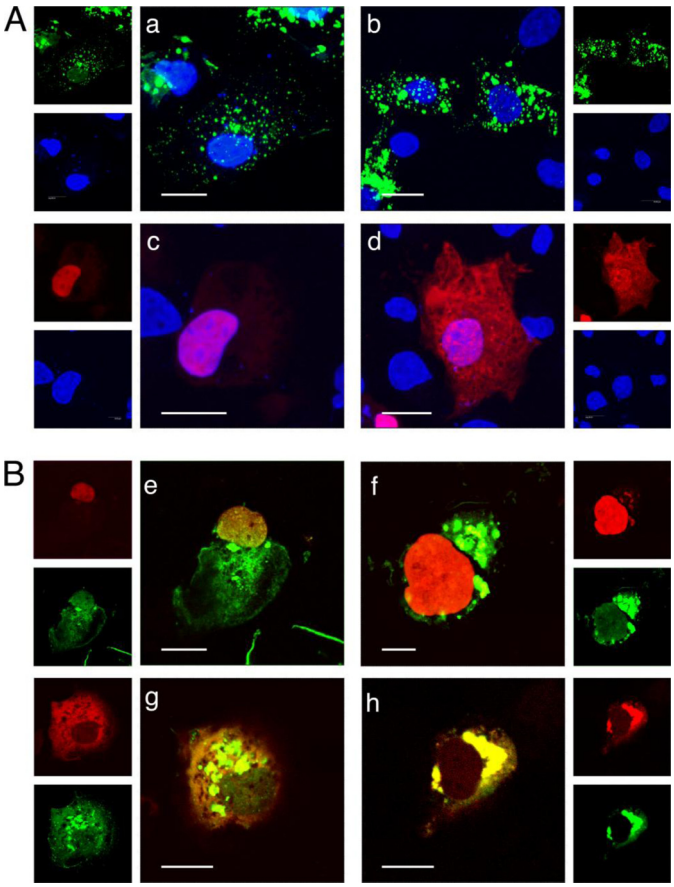

FIGURE 5. **Colocalization of β-dystrobrevin and iBRAF in transfected COS-7 cells.** *A*, the subcellular distribution of iBRAF and β-dystrobrevin was determined by transfecting COS-7 cells with pEGFP/β-DB (*a* and *b*) and pDsRed-C1/iBRAF (*c* and *d*), respectively. β-Dystrobrevin (*green*) is located in intensely stained punctae distributed throughout the cytoplasm (*a* and *b*) and is expressed in many nuclei (*a, upper inset*), whereas iBRAF (*red*) appears to be a nuclear protein (*c* and *d*) that can also be found in the cytoplasm (*d*). Nuclear staining was by Hoechst (*blue*). *B*, coexpression of β-dystrobrevin and iBRAF resulted in a significant colocalization in the nucleus (*e* and *f*) as well as in the cytoplasm (*g* and *h*), although the amount of their relative expression in the same cellular compartment may be quite different (*f*, see the *insets*). Merged images are shown in *a-h*, single fluorescence in the side *insets*. *Scale bar*, 10 μm.

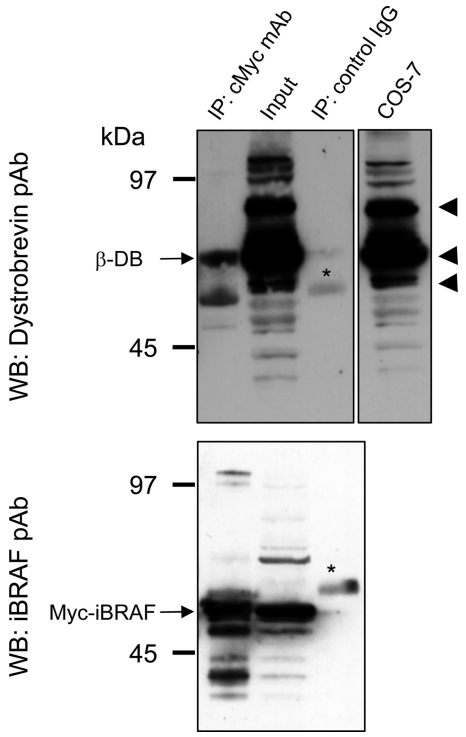

FIGURE 6. **Interaction of β-dystrobrevin and iBRAF in COS-7 cells transfected with pCMV-Myc/iBRAF.** Anti-cMyc immunoprecipitate (*IP: cMyc mAb*), COS-7 transfected cell lysate (*input*), and mouse IgG control immunoprecipitate (*IP: control IgG*) were separated by SDS-PAGE, and transferred to nitrocellulose. The blot was probed with polyclonal anti-β-dystrobrevin and anti-iBRAF antibodies (*pAb*) and revealed by ECL. The cMyc monoclonal antibody co-immunoprecipitates β-dystrobrevin and iBRAF (*arrows*). The *asterisks* indicate IgG heavy chains, *arrowheads* indicate the bands corresponding to the major dystrobrevin isoforms (α-dystrobrevin 1, 78 kDa; β-dystrobrevin, 59 kDa; α-dystrobrevin 2, 55 kDa). Molecular mass markers are indicated at the left (*kDa*). *WB*, Western blot.

HMG20 Proteins Associate with Members of the Dystrophin Family—Besides iBRAF/HMG20a, the HMG20 class of proteins comprises a second member, BRAF35/HMH20b (35), a component of the co-repressor BRAF35-HDAC complex involved in the repression of neuronal specific genes in non-neuronal tissue and neuronal progenitors (32). Because BRAF35 is highly homologous to iBRAF, we carried out pulldown experiments using recombinant GST-BRAF35 and *in vitro* transcribed/translated β-dystrobrevin to verify the existence of an interaction between these proteins and found that GST-BRAF35 directly binds ^{35}S-labeled β-dystrobrevin (Fig. 9*A*). We, therefore, used the same strategy as in the case of β-dystrobrevin and iBRAF to further characterize the interaction of BRAF35 with β-dystrobrevin. SPR analysis indeed revealed that the β-dystrobrevin amino-terminal region is involved in the interaction with BRAF35, and pulldown assays showed that a binding site for β-dystrobrevin lies on the BRAF35 carboxyl-terminal region (data not shown). Furthermore, we evaluated by SPR the dissociation constant K_d of the β-dystrobrevin interaction with BRAF35 and found it of the same order of magnitude (70–90 nM) (data not shown) as that with iBRAF. Co-precipitation experiments on lysates from HeLa, P19, and NTera-2 cells followed by Western blot with a monoclonal BRAF35 antibody revealed that BRAF35 was immunoprecipitated by the monoclonal dystrobrevin antibody (Fig. 9*B*), suggesting that the interaction of β-dystrobrevin and BRAF35 also occurs *in vivo*.

As members of the dystrophin family, dystrobrevins share high sequence homology with the carboxyl-terminal tail of dystrophin. Recently, the short dystrophin isoform Dp71 has been revealed in the nuclei of different cell types, where it has been suggested it may work as a scaffolding protein involved in nuclear architecture and modulation of nuclear processes (36–38). We decided to investigate whether Dp71 interacts with the HMG20 proteins iBRAF and BRAF35 and to this aim performed pulldown experiments with recombinant proteins. We found that both His_6-iBRAF (Fig. 9*C*, *left*) and GST-BRAF35 (Fig. 9*C*, *right*) directly bind to ^{35}S-labeled Dp71, whereas no interaction was detected with the appropriate negative controls.

DISCUSSION

Here, we have identified iBRAF/HMG20a and BRAF35/HMG20b as new β-dystrobrevin-associated proteins. iBRAF

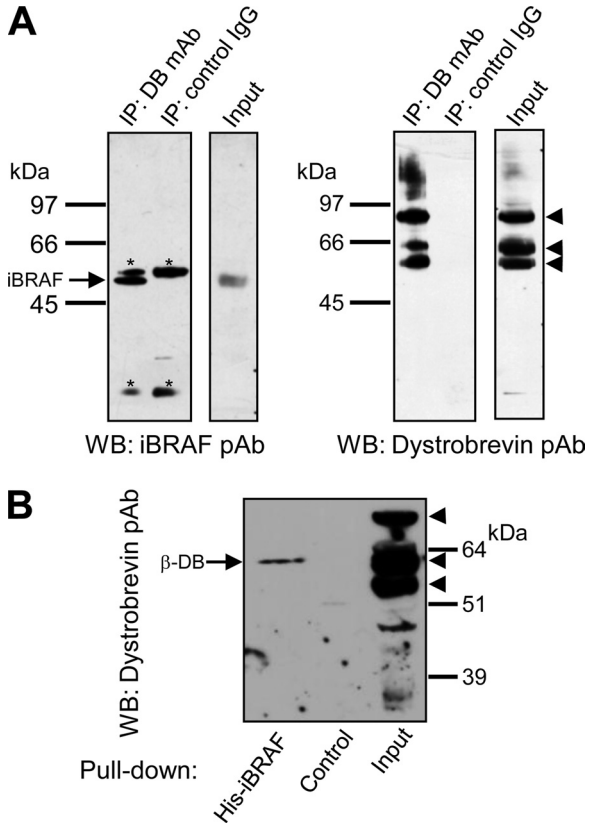

FIGURE 7. **Direct interaction of β-dystrobrevin and iBRAF in rat brain.** *A*, immunoprecipitation is shown. The monoclonal anti-dystrobrevin antibody co-immunoprecipitates iBRAF with dystrobrevin isoforms. Anti-dystrobrevin immunoprecipitate (*IP: DB mAb*), mouse IgG control immunoprecipitate (*IP: control IgG*), and rat brain lysate (*Input*) were separated by SDS-PAGE and transferred to nitrocellulose. The blot was probed with the polyclonal anti-β-dystrobrevin and iBRAF antibodies (*pAb*) and revealed by ECL. *Asterisks*, IgG heavy and light chains; *arrow*, iBRAF; *arrowheads*, major dystrobrevin isoforms (α-dystrobrevin 1, 78 kDa; β-dystrobrevin, 59 kDa; α-dystrobrevin 2, 55 kDa). Molecular mass markers are indicated at the left (*kDa*). *WB*, Western blot. *B*, pulldown is shown. Rat brain lysate was incubated with His_6-iBRAF prebound to Ni-NTA-agarose beads (*His-iBRAF*) or beads alone (*Control*). After extensive washing, bound proteins were separated by SDS-PAGE and transferred to nitrocellulose. The blot was probed with polyclonal anti-β-dystrobrevin antibody and revealed by ECL. Bands corresponding to major dystrobrevin isoforms are indicated by the *arrowheads* at the *right*. Molecular mass markers are indicated at the *right* (*kDa*).

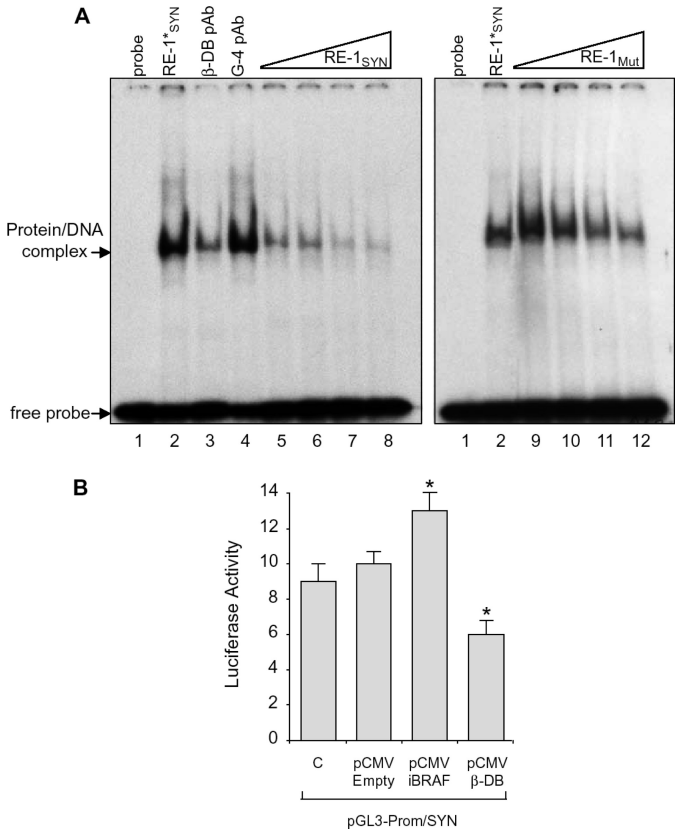

FIGURE 8. **β-Dystrobrevin binds to RE-1 and represses the synapsin I promoter.** *A*, electrophoretic mobility shift assays are shown. Nuclear extracts from NTera-2 cells after 4 days of retinoic acid treatment were used in band shift experiments. A ^{32}P-labeled double-strand oligonucleotide containing the synapsin RE-1 element ($RE\text{-}1^{*}_{syn}$) was used as a probe. The protein-DNA complex was revealed in *lane 2*. The positions of migration of the free probe and the specific protein-DNA complex are indicated by *arrows*. Supershift experiments were conducted by addition of anti-β-dystrobrevin (*β-DB pAb*; *lane 3*) or anti-GATA-4 (*G-4 pAb*; *lane 4*) antibodies. Competitive experiments were performed using a 50-, 100-, 300-, and 600-fold molar excess of either the unlabeled oligonucleotide $RE\text{-}1_{SYN}$ (*lanes 5–8*) or the unlabeled mutated oligonucleotide $RE\text{-}1_{Mut}$ (*lanes 9–12*). *B*, promoter activity assay is shown. *pGL3-Prom/SYN*, a fragment of the human synapsin promoter sequence including the RE-1 element (*SYN*) subcloned in a firefly luciferase vector containing a minimal promoter (*pGL3-Prom*) was co-transfected with a *Renilla* luciferase vector as an internal control for normalization and with a pCMV-Myc expression vector for iBRAF (*pCMV-iBRAF*) or for β-DB (*pCMV-βDB*), as compared with the empty pCMV-Myc vector (*pCMV-Empty*). *C*, control, no pCMV. Data are the mean ± S.E. values of three independent experiments; *, $p < 0.05$, compared with *C* or *pCMV-Empty* controls.

and BRAF35 are members of the HMG-box proteins, a group of ubiquitous non-histone chromosomal factors that affect chromatin dynamics. The HMG box that identifies this family consists of a conserved DNA binding domain involved in the regulation of transcription and chromatin conformation (39). Outside of this domain, the HMG20 proteins iBRAF/HMG20a and BRAF35/HMG20b lack any significant homology to other known proteins, thus defining a distinct class of mammalian HMG-box proteins (35). iBRAF and BRAF35 indeed share 70% identity within the HMG-box and 57% within the carboxyl-terminal coiled-coil domain (33). It was reported that iBRAF (for inhibitor of BRAF35) overcomes the repressive effects of the neuronal silencer REST and activates REST-responsive genes through the modulation of histone methylation (33). In contrast to BRAF35, which is a component of the BRAF35-HDAC complex co-repressor complex required for the repression of REST-responsive genes (40), iBRAF expression leads to the abrogation of REST-mediated transcriptional repression and the consequent activation of the neuronal differentiation program (33).

Using a combination of yeast two-hybrid analysis, co-precipitation *in vitro* and from cell and brain extracts, and colocalization in transfected cells, we have obtained evidence that β-dystrobrevin directly interacts with iBRAF. By assessing the kinetics of the interaction through SPR analysis, we also found that β-dystrobrevin and iBRAF interact with high affinity ($K_d \approx$ 30 nM). Furthermore, we localized the binding region of each protein on the other and determined that a β-dystrobrevin binding site on iBRAF lies in the carboxyl-terminal part of iBRAF, within amino acids 233 and 342, and the iBRAF binding site on β-dystrobrevin in the amino-terminal region of β-dystrobrevin, within amino acids 1 and 352. Although both β-dystrobrevin and iBRAF contain coiled-coil domains, their associ-

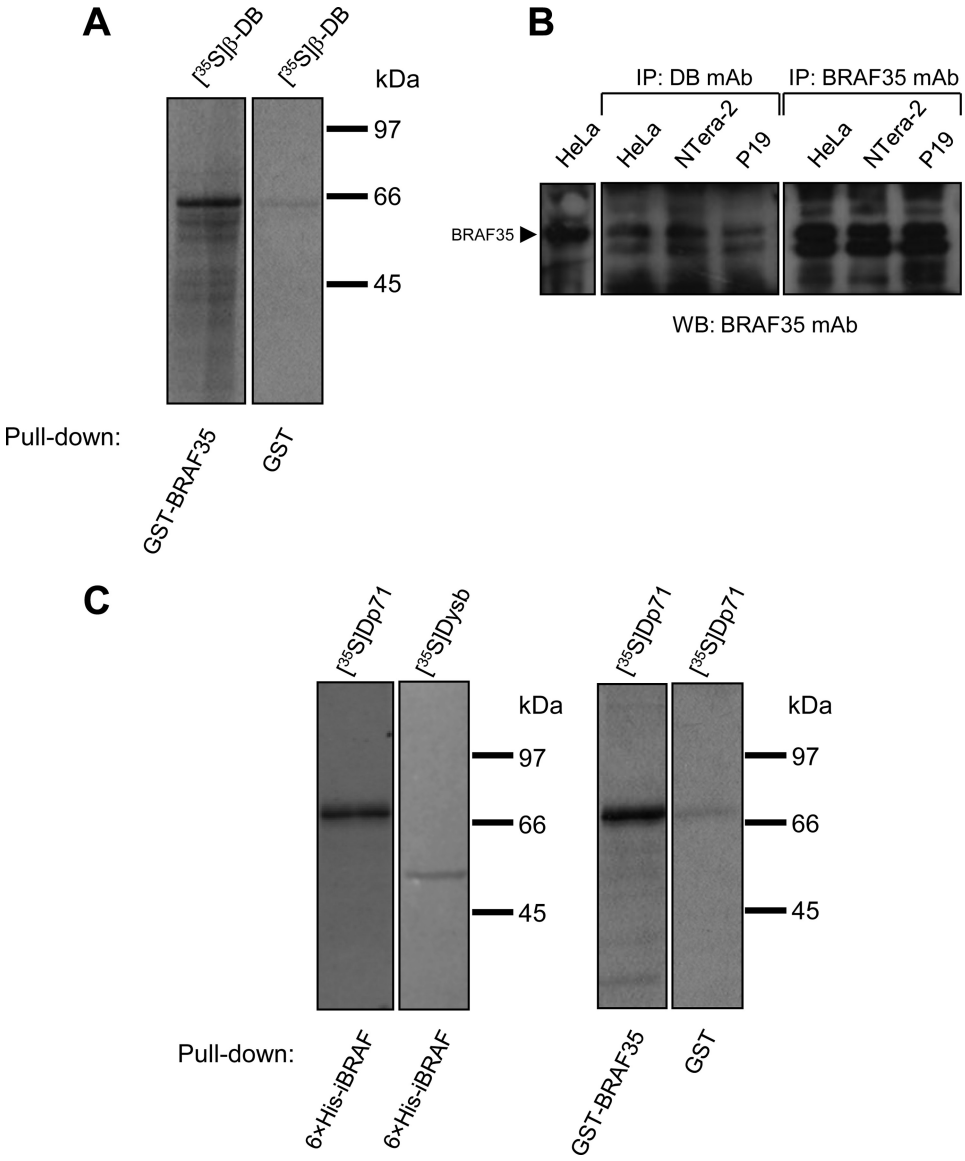

FIGURE 9. **HMG20 proteins associates with members of the dystrophin family.** *A*, binding of ^{35}S-labeled-β-dystrobrevin (*β-DB*) to immobilized *GST-BRAF35* is shown. Pulled-down proteins were analyzed by SDS-PAGE and detected by autoradiography. Molecular mass markers are indicated at the *right* (*kDa*). *B*, the anti-dystrobrevin monoclonal antibody co-immunoprecipitates BRAF35 from cultured cells. Proteins immunoprecipitated from HeLa, NTera-2, and P19 cells by anti-dystrobrevin (*IP: DB mAb*) and anti-BRAF35 (*IP: BRAF35 mAb*) antibodies were separated by SDS-PAGE and transferred to nitrocellulose. The blot was probed with the monoclonal BRAF35 antibody and revealed by ECL. The position of the band corresponding to BRAF35 is indicated by an *arrowhead* at the *left*. A *lower band* is detectable in all immunoprecipitates: its absence in HeLa cell lysate input (*HeLa*; positive control) suggests that it represents most likely a degradation product. *C*, both iBRAF and BRAF35 interact with dystrophin short isoform Dp71 *in vitro*. Binding of ^{35}S-labeled Dp71 to immobilized iBRAF (6 x His-*iBRAF*; *left*) and to immobilized BRAF35 (*GST-BRAF35*; *right*) is shown. ^{35}S-Labeled dysbindin (*Dysb*; *left*) and GST protein (*GST*; *right*) were used as negative controls, respectively. Samples were pulled down by the appropriate tagged proteins, analyzed by SDS-PAGE, and detected by autoradiography. Molecular mass markers are indicated at the right (*kDa*).

ation is not mediated by them. In fact, although the carboxyl-terminal region of iBRAF that interacts with β-dystrobrevin contains a coiled-coil domain, coiled-coil domains are not included in the binding region of β-dystrobrevin.

To get insights into the *in vivo* association of β-dystrobrevin with iBRAF, we have followed their interaction through direct fluorescence in eukaryotic-transfected cells. We found that in many single transfected COS-7 cells, both proteins distributed in the nucleus as well as in the cytoplasm. Although dystrobrevin, at first considered a cytoplasmic component of the DPC, has already been described in the nuclear compartment (37, 41), iBRAF was so far regarded essentially as a nuclear protein (35). Our confocal microscopy results show that iBRAF and β-dystrobrevin colocalize in the nucleus as well as in the cytoplasm of co-transfected cells. Further evidence of the interaction of β-dystrobrevin and iBRAF *in vivo* comes from co-immunoprecipitation data obtained from COS-7-transfected cells and rat brain homogenates. We found that iBRAF and β-dystrobrevin co-precipitated in the same complex, whereas α-dystrobrevin did not, suggesting that iBRAF specifically interacts with the β isoform of dystrobrevin. Our co-immunoprecipitation data are strengthened by pulldown results obtained using His_6-iBRAF to co-precipitate iBRAF and its associated proteins from rat brain extracts. These data match our *in vitro* results showing that the presence of β-dystrobrevin and iBRAF in the same complex was due to direct interaction.

Information on protein-protein interaction provides valuable insight into the mechanisms underlying protein functions. Our characterization of β-dystrobrevin association with iBRAF suggests the possibility that β-dystrobrevin plays a role in chromatin remodeling events that lead to initiation of neuronal differentiation. A possible involvement of β-dystrobrevin isoform in neurogenesis and brain development has already been suggested by its interaction with the extracellular matrix protein pancortin (21), which is thought to play a role in neuronal differentiation and survival (22). The specific interaction with iBRAF, an HMG-domain protein with a key function in the initiation of neuronal gene transcription, therefore strengthens the hypothesis of the involvement of β-dystrobrevin in these processes.

iBRAF RNA is widely expressed in mouse developing brain (33) and throughout the mature human brain, with the higher levels being found in the cerebellum (35). In the rat brain, α- and β-dystrobrevin are differentially expressed; α-dystrobrevin-1 is present in perivascular astrocytes and in Bergmann glia

of the cerebellum, whereas β-dystrobrevin is found in the hippocampal, cortical, and cerebellar neurons (41), where iBRAF expression leads to the abrogation of the repressive effects of the neuronal silencer REST. It seems likely that an association between iBRAF and the β isoform, rather than the α isoform of dystrobrevin, has developed and that this association has a functional significance.

Here we also found evidence that BRAF35 behaves similarly to iBRAF in its binding to β-dystrobrevin. BRAF35 is a component of the BRAF35-HDAC complex that mediates the repression of neuron-specific genes, and it has been suggested that BRAF35 regulates gene expression through remodeling of chromatin structure (40). Our band shift experiments indicate that β-dystrobrevin participates in protein complexes that bind to RE-1 in the promoter of neuronal genes, and luciferase assays show that β-dystrobrevin acts as a repressor of the synapsin promoter activity after direct binding to RE-1. Reports from our and other laboratories (for review, see Ref. 42) designate dystrobrevin as a multifunctional scaffold protein with functions in different cell processes. Considering that iBRAF and BRAF35 play opposite roles in the transcriptional regulation of neuronal genes (33), β-dystrobrevin may work as a scaffolding protein involved both in the activation and in the repression of neuron-specific genes.

Moreover, we also show that dystrobrevin-interacting dystrophin short isoform Dp71 interacts with both iBRAF and BRAF35 *in vitro*. Nuclear DPC components, including Dp71 and β-dystrobrevin, have been found in HeLa cells associated with the nuclear matrix, indicating that members of the nuclear DPC may work as scaffolding proteins involved in nuclear architecture (37). It has been reported that Dp71 binding to the nuclear matrix is modulated during neuronal differentiation (43), that Dp71 expression is induced during development of the nervous system (44, 45), and that Dp71 deficit appears as a worsening factor of the cognitive impairment associated with Duchenne and Becker muscular dystrophy (46). The results of our study open a new way of looking at the DPC components β-dystrobrevin and Dp71. The interaction of these proteins with the chromatin remodeling proteins iBRAF and BRAF35 suggests that nuclear DPC components may be involved in the epigenetic processes that regulate gene expression, opening a new scenario that would help in understanding the molecular mechanisms underlying the neuronal involvement in DMD. Further studies are necessary to identify which genes are regulated by the chromatin remodeling events in which these proteins may be implicated.

Acknowledgments—We are indebted to Caterina Veroni for her contribution during the preliminary phases of the project. We are grateful to Carlo Ramoni and Lucia Gaddini for collaboration. We also thank Giuseppe Loreto and Massimo Delle Femmine for help with the graphics.

REFERENCES

1. Ervasti, J. M., and Campbell, K. P. (1993) *J. Cell Biol.* **122,** 809–823
2. Rando, T. A. (2001) *Muscle Nerve* **24,** 1575–1594
3. Blake, D. J., Weir, A., Newey, S. E., and Davies, K. E. (2002) *Physiol. Rev.* **82,** 291–329
4. Waite, A., Tinsley, C. L., Locke, M., and Blake, D. J. (2009) *Ann. Med.* **41,** 344–359
5. Moizard, M. P., Billard, C., Toutain, A., Berret, F., Marmin, N., and Moraine, C. (1998) *Am. J. Med. Genet.* **80,** 32–41
6. Cyrulnik, S. E., and Hinton, V. J. (2008) *Neurosci. Biobehav. Rev.* **32,** 486–496
7. Ambrose, H. J., Blake, D. J., Nawrotzki, R. A., and Davies, K. E. (1997) *Genomics* **39,** 359–369
8. Loh, N. Y., Ambrose, H. J., Guay-Woodford, L. M., DasGupta, S., Nawrotzki, R. A., Blake, D. J., and Davies, K. E. (1998) *Mamm. Genome* **9,** 857–862
9. Blake, D. J., Nawrotzki, R., Peters, M. F., Froehner, S. C., and Davies, K. E. (1996) *J. Biol. Chem.* **271,** 7802–7810
10. Blake, D. J., Nawrotzki, R., Loh, N. Y., Górecki, D. C., and Davies, K. E. (1998) *Proc. Natl. Acad. Sci. U.S.A.* **95,** 241–246
11. Peters, M. F., O'Brien, K. F., Sadoulet-Puccio, H. M., Kunkel, L. M., Adams, M. E., and Froehner, S. C. (1997) *J. Biol. Chem.* **272,** 31561–31569
12. Sadoulet-Puccio, H. M., Khurana, T. S., Cohen, J. B., and Kunkel, L. M. (1996) *Hum. Mol. Genet.* **5,** 489–496
13. Grady, R. M., Grange, R. W., Lau, K. S., Maimone, M. M., Nichol, M. C., Stull, J. T., and Sanes, J. R. (1999) *Nat. Cell Biol.* **1,** 215–220
14. Loh, N. Y., Nebenius-Oosthuizen, D., Blake, D. J., Smith, A. J., and Davies, K. E. (2001) *Mol. Cell. Biol.* **21,** 7442–7448
15. Grady, R. M., Wozniak, D. F., Ohlemiller, K. K., and Sanes, J. R. (2006) *J. Neurosci.* **26,** 2841–2851
16. Benson, M. A., Newey, S. E., Martin-Rendon, E., Hawkes, R., and Blake, D. J. (2001) *J. Biol. Chem.* **276,** 24232–24241
17. Macioce, P., Gambara, G., Bernassola, M., Gaddini, L., Torreri, P., Macchia, G., Ramoni, C., Ceccarini, M., and Petrucci, T. C. (2003) *J. Cell Sci.* **116,** 4847–4856
18. Ceccarini, M., Torreri, P., Lombardi, D. G., Macchia, G., Macioce, P., and Petrucci, T. C. (2005) *J. Mol. Biol.* **354,** 872–882
19. Albrecht, D. E., and Froehner, S. C. (2004) *J. Biol. Chem.* **279,** 7014–7023
20. Ceccarini, M., Grasso, M., Veroni, C., Gambara, G., Artegiani, B., Macchia, G., Ramoni, C., Torreri, P., Mallozzi, C., Petrucci, T. C., and Macioce, P. (2007) *J. Mol. Biol.* **371,** 1174–1187
21. Veroni, C., Grasso, M., Macchia, G., Ramoni, C., Ceccarini, M., Petrucci, T. C., and Macioce, P. (2007) *J. Neurosci. Res.* **85,** 2631–2639
22. Nagano, T., Nakamura, A., Konno, D., Kurata, M., Yagi, H., and Sato, M. (2000) *J. Neurochem.* **75,** 1–8
23. Benson, M. A., Sillitoe, R. V., and Blake, D. J. (2004) *Trends Neurosci.* **27,** 516–519
24. Bianchi, M. E., and Agresti, A. (2005) *Curr. Opin. Genet. Dev.* **15,** 496–506
25. Ceccarini, M., Rizzo, G., Rosa, G., Chelucci, C., Macioce, P., and Petrucci, T. C. (1997) *Brain Res. Dev. Brain Res.* **103,** 77–82
26. Jüngling, S., Cibelli, G., Czardybon, M., Gerdes, H. H., and Thiel, G. (1994) *Eur. J. Biochem.* **226,** 925–935
27. Russo, K., Di Stasio, E., Macchia, G., Rosa, G., Brancaccio, A., and Petrucci, T. C. (2000) *Biochem. Biophys. Res. Commun.* **274,** 93–98
28. Cianetti, L., Di Cristofaro, A., Zappavigna, V., Bottero, L., Boccoli, G., Testa, U., Russo, G., Boncinelli, E., and Peschle, C. (1990) *Nucleic Acids Res.* **18,** 4361–4368
29. Ceccarini, M., Macioce, P., Panetta, B., and Petrucci, T. C. (2002) *Neuromuscul. Disord.* **12,** 36–48
30. Labbaye, C., Quaranta, M. T., Pagliuca, A., Militi, S., Licht, J. D., Testa, U., and Peschle, C. (2002) *Oncogene* **21,** 6669–6679
31. Schoch, S., Cibelli, G., and Thiel, G. (1996) *J. Biol. Chem.* **271,** 3317–3323
32. Ballas, N., and Mandel, G. (2005) *Curr. Opin. Neurobiol.* **15,** 500–506
33. Wynder, C., Hakimi, M. A., Epstein, J. A., Shilatifard, A., and Shiekhattar, R. (2005) *Nat. Cell Biol.* **7,** 1113–1117
34. Hsiao, J. C., Chao, C. C., Young, M. J., Chang, Y. T., Cho, E. C., and Chang, W. (2006) *J. Virol.* **80,** 7714–7728
35. Sumoy, L., Carim, L., Escarceller, M., Nadal, M., Gratacòs, M., Pujana, M. A., Estivill, X., and Peral, B. (2000) *Cytogenet. Cell Genet.* **88,** 62–67
36. Marquez, F. G., Cisneros, B., Garcia, F., Ceja, V., Velázquez, F., Depardón, F., Cervantes, L., Rendón, A., Mornet, D., Rosas-vargas, H., Mustre, M., and Montañez, C. (2003) *Neuroscience* **118,** 957–966

37. Fuentes-Mera, L., Rodríguez-Muñoz, R., González-Ramírez, R., García-Sierra, F., González, E., Mornet, D., and Cisneros, B. (2006) *Exp. Cell Res.* **312,** 3023–3035
38. González-Ramírez, R., Morales-Lázaro, S. L., Tapia-Ramírez, V., Mornet, D., and Cisneros, B. (2008) *J. Cell. Biochem.* **105,** 735–745
39. Travers, A. A. (2003) *EMBO Rep.* **4,** 131–136
40. Hakimi, M. A., Bochar, D. A., Chenoweth, J., Lane, W. S., Mandel, G., and Shiekhattar, R. (2002) *Proc. Natl. Acad. Sci. U.S.A.* **99,** 7420–7425
41. Blake, D. J., Hawkes, R., Benson, M. A., and Beesley, P. W. (1999) *J. Cell Biol.* **147,** 645–658
42. Rees, M. L., Lien, C. F., and Górecki, D. C. (2007) *Neuromuscul. Disord.* **17,** 123–134
43. Rodríguez-Muñoz, R., Villarreal-Silva, M., González-Ramírez, R., García-Sierra, F., Mondragón, M., Mondragón, R., Cerna, J., and Cisneros, B. (2008) *Biochem. Biophys. Res. Commun.* **375,** 303–307
44. Jung, D., Filliol, D., Metz-Boutigue, M. H., and Rendon, A. (1993) *Neuromuscul. Disord.* **3,** 515–518
45. Sarig, R., Mezger-Lallemand, V., Gitelman, I., Davis, C., Fuchs, O., Yaffe, D., and Nudel, U. (1999) *Hum. Mol. Genet.* **8,** 1–10
46. Daoud, F., Angeard, N., Demerre, B., Martie, I., Benyaou, R., Leturcq, F., Cossée, M., Deburgrave, N., Saillour, Y., Tuffery, S., Urtizberea, A., Toutain, A., Echenne, B., Frischman, M., Mayer, M., Desguerre, I., Estournet, B., Réveillère, C., Penisson-Besnier, Cuisset, J. M., Kaplan, J. C., Héron, D., Rivier, F., and Chelly, J. (2009) *Hum. Mol. Genet.* **18,** 3779–3794